Ternary Al–Ni–Er System

Subjects: Materials Science, Characterization & Testing

Contributor: Qian Song, Chenbo Li, Zixuan Deng, Ligang Zhang, Libin Liu

Al–Ni–Er is an essential system in heat-resistant Al alloys. The aluminum-rich corner of this system, which has the most practical application significance. The phase equilibria of the Al–Ni–Er system are investigated via experiments and thermodynamic modeling. The isothermal sections of the Al-rich corner of this ternary system at 600 and 700 °C were determined through equilibrated alloys combined with scanning electron microscopy (SEM), electron probe microanalysis (EPMA) and X-ray diffractometry (XRD).

Keywords: Al–Ni–Er system ; equilibrated alloys ; isothermal sections

1. Introduction

Aluminum alloys have a history of nearly a century, but they have developed rapidly. The addition of nickel in aluminum alloys offers higher tensile strength and hardness, greatly improves corrosion resistance [1], and has high specific strength that could effectively reduce the weight of products, lower fuel consumption, and save energy in industrial production [2][3]. It can also promote a reduction in carbon emissions and help in achieving carbon neutrality [4]. The amorphous aluminum alloy has better properties than those of ordinary aluminum alloys. The glass-forming ability (GFA) of Al alloys could be promoted with the addition of rare earth metals (REs) [5][6][7]. Through a comprehensive consideration of cost and performance, the researchers chose the Al–Ni–Er system as the research object.

Phase diagrams and thermodynamics are powerful tools applied to material design [8][9][10][11]. CALPHAD is a more efficient method than experimental research because an experiment cannot cover all points in a 3D phase diagram model, and CALPHAD can obtain comprehensive information that can guide the experiment. Al–Ni–Er is an essential system in heat-resistant Al alloys. Studying its thermodynamics can not only guide the design of Al–Ni–Er alloys, but also supplement the database of Al-based alloys.

2. Binary Al–Ni System

In 1993, Okamoto [12] revised Nash's [13] evaluation of the binary Al–Ni system, and rereported the experimental phase diagram of the system. The binary Al–Ni phase diagram evaluated by Okamoto is the generally accepted version. In the binary Al–Ni system, there are two terminal solid solutions with an FCC structure, the three intermetallic compounds of $NiAl_3$, Ni_2Al_3, and Ni_5Al_3, and an NiAl phase with a B2-ordered structure and an Ni_3Al phase with an $L1_2$-ordered structure. AlNi, Al_3Ni_2, and $AlNi_3$ had a certain range of solid solubility at 600 and 700 °C [14].

Since Gwyer [15] initiated his work, many experiments have been carried out to determine the phase equilibrium and thermodynamic quantities of the Al–Ni system. Kaufman, and Nesor and Ansara et al. [16] produced a thermodynamic model of the whole system through phase diagram calculation. Then, Du [17], Ansara [16], Huang [18], Dupin [19], Lu [20], and Chen [21] used different models to optimize this system. The calculated phase diagram and thermodynamic description of Al–Ni were also constantly updated. The final thermodynamic model and parameters of Al–Ni binary system can be found in the thermodynamic simulation of the ternary Al–Cr–Ni system by Dupin et al. [19]. **Figure 1** is the Al–Ni binary phase diagram drawn according to the thermodynamic parameters in the literature.

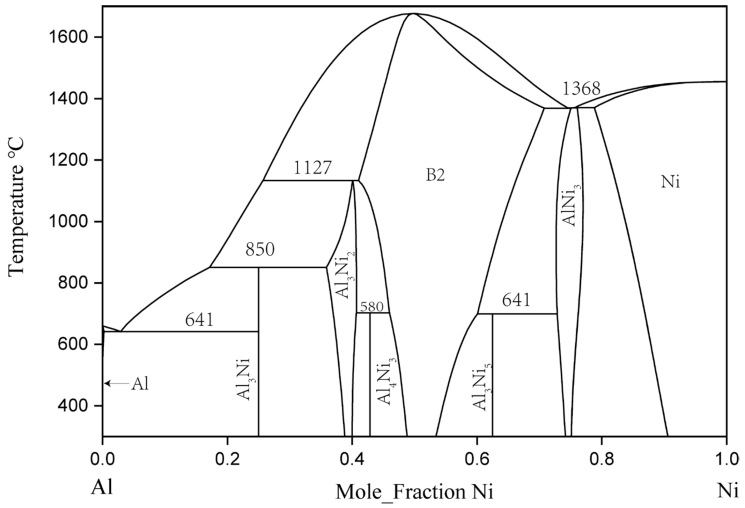

Figure 1. Al–Ni phase diagram [14][22].

3. Binary Er–Ni System

The phase equilibrium relation of the binary Er–Ni system was first studied by Buschow [23] in 1968. In total, 11 intermetallic compounds were identified: $ErNi_3$, Er_2Ni_7, $ErNi_4$, Er_4Ni_{17}, Er_5Ni_{22}, $ErNi_5$, Er_2Ni_{17}, Er_3Ni, Er_5Ni_3, ErNi, and $ErNi_2$. In 1974, Moreau et al. [24] studied the Er_3Ni_2 compound and found that Er_5Ni_3 should be replaced by Er_3Ni_2. Subsequently, in 1999, Du et al. [25] used the CALPHAD method to assess thermodynamic parameters and established a comprehensive thermodynamic database of this binary system. The phase diagram of the Er–Ni binary system calculated by Du et al. is shown in **Figure 2** [25].

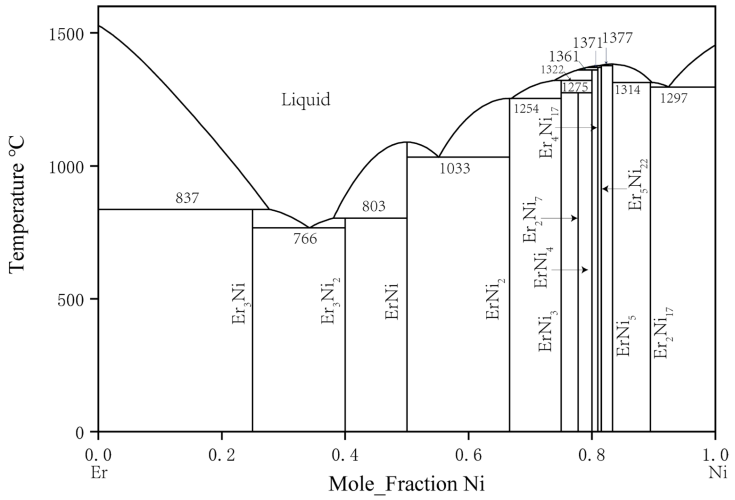

Figure 2. Er–Ni phase diagram assessed by Du et al. [25].

4. Binary Al–Er System

In 1965, The binary Al–Er system was first studied by Buschow and Vucht [26]. They discovered $AlEr_2$, Al_2Er_3, AlEr, Al_2Er, and Al_3Er. Their study indicated that the solid solubility of Al in Er was close to 8 at. % at 860 °C, which seemed unusually high. In 1988, Gschneidner and Calderwood [27] restudied this system. Considering the 23% size difference between Er and Al, the actual solid solubility had to be less than 1 at. %. The previous observation might have been due to an impurity effect or nonequilibrium conditions. However, in their results, the curvature change in the liquidus curve did not conform to convention in the 50 to 80 at. % Er composition range. In 2002, Cacciamani et al. [28] conducted thermodynamic modeling and optimization for the Al–Er system, and their Al–Er phase diagram is shown in **Figure 3**. In 2022, L Xu et al., thermodynamically assessed this system [29].

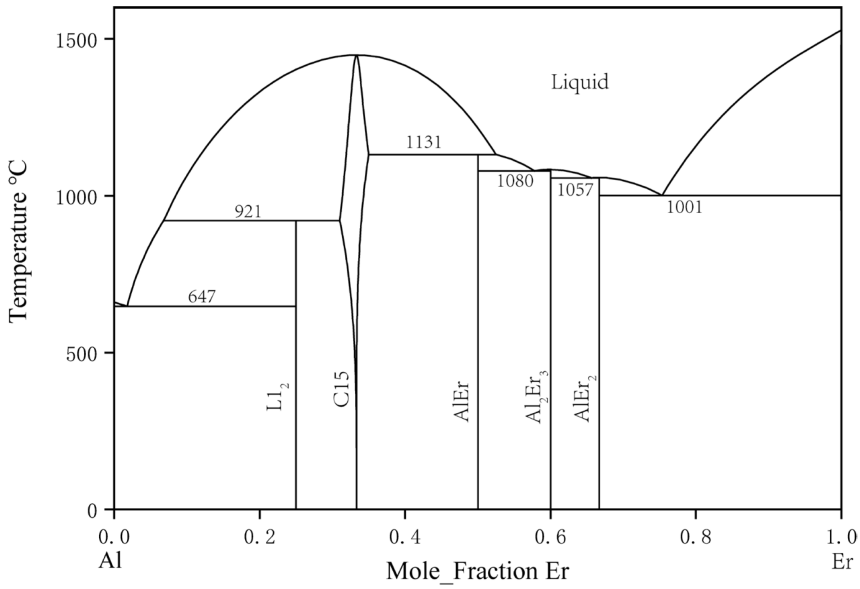

Figure 3. Calculated Al–Er phase diagram by Cacciamani et al. [28].

5. Ternary Al–Ni–Er System

There is relatively little information about the ternary Al–Ni–Er system. In 1982, Zarechnyuk et al. [30] first reported that the Er content in this system was 0–33 at. %. At the isothermal cross section at 800 °C, nine intermediate compounds were determined: τ4–Al_4NiEr, τ5–$Al_{3-x}Ni_{2+x}Er$, τ6–Al_2NiEr, τ7–$AlNi_8Er_3$, τ8–$Al_2Ni_6Er_3$, τ9–$AlNi_2Er_2$, τ10–AlNiEr, $Al_7Ni_3Er_2$, and $Al_{16}Ni_3Er$. Combined with the later findings regarding the τ2–Al_9Ni_3Er phase, the Al_2Ni_3Er phase was reported by Gladyshevskii [31], and Sorgic et al. [32]. Riccardo et al. [33] drew a relatively complete isothermal section phase diagram of the ternary Al–Ni–Er system at 800 °C, as shown in **Figure 4**.

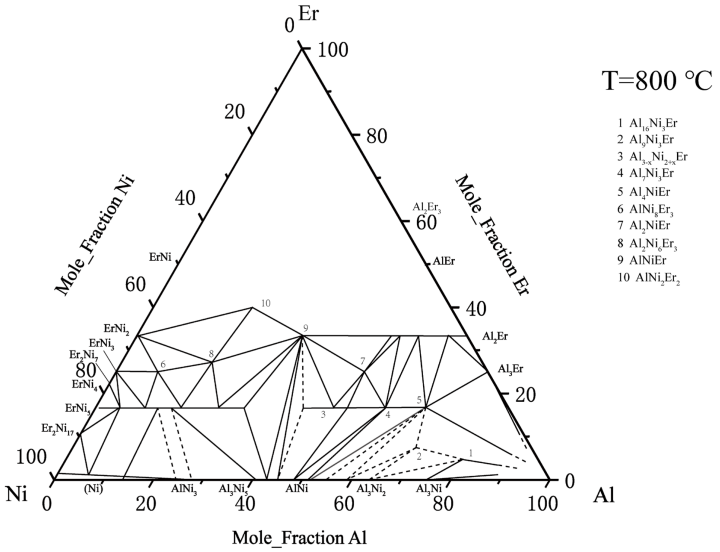

Figure 4. Al–Ni–Er phase diagram assessed by Riccardo et al. [33].

On the basis of the above research, Zhao et al. [34] used the equilibrium alloy method to determine most of the phase diagram of the ternary Al–Ni–Er system at 600 °C with Er content from 0 to 67 at. %. Three new ternary mesophase, namely, $AlNiEr_4$, $AlNi_6Er_{13}$ and $AlNi_2Er$ were named τ11, τ12, and τ13. Because the pure phase was not obtained in the experiment, the structures of these ternary compounds were not discussed. The above work also revised $ErNi_5$ τ5. Al_2Er, $ErNi_2$, and τ10. The isothermal section of the ternary Al–Ni–Er system at 600 °C was drawn as shown in **Figure 5**.

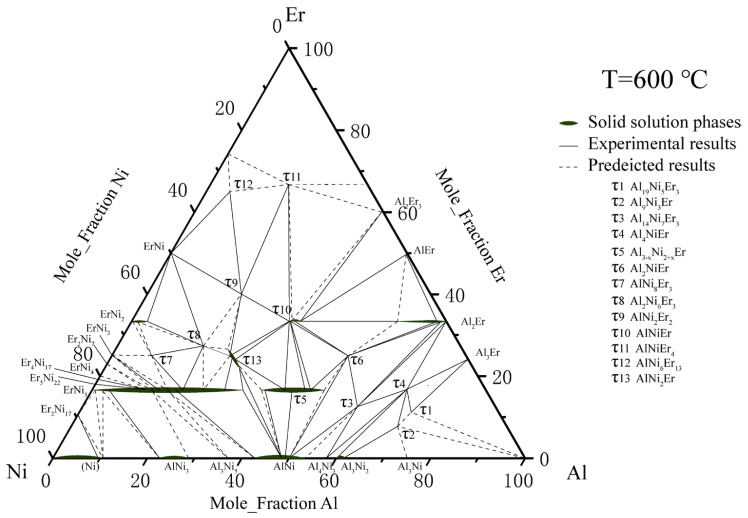

Figure 5. Al–Ni–Er phase diagram assessed by Zhao et al. [34].

Similarly, Zhao et al. measured the isothermal section of the Al–Ni–Er system at 700 °C and 6 phase zones at the Al-rich corner: Al_2Er + Al_3Er + τ4, Al + τ1 + τ2, Al + τ2 + Al_3Ni, Al_3Ni_2 + τ2 + Al_3Ni, Al + τ1 + Al_3Er, and τ1 + Al_3Er + τ4. At the Al-rich corner (60–100% Al) of the experimental phase diagram of the ternary Al–Ni–Er alloy, at the margin, there were four ternary intermetallic compounds, namely, τ1, τ2, τ3, τ4, and four binary compounds, Al_3Ni_2, Al_3Ni, Al_2Er and Al_3Er.

According to the literature research, Al_2Er should show a certain solid solubility to Ni in a parallel direction to Er. The ideal stoichiometric composition, solid-phase crystal structure, and lattice parameters of the above compounds could be obtained by investigating the existing literature data, as shown in **Table 1**.

Table 1. Crystallographic data of all phases in the Al–Ni–Er system.

System	Phase	Prototype	Pearson Symbol	Lattice Parameters (nm)			Refs.
				a	b	c	
Al	Fcc_A1, (Al)	Cu	cF4	0.40496			[35]
Ni	Fcc_A1, (Ni)	Cu	cF4	0.3524			[35]
Er	Hcp_A3, (Er)	Mg	hP2	0.359		0.555	[35]
Al–Ni	Al3Ni	Al3Ni	oP16	0.6613	0.7367	0.4811	[36]
	Al3Ni2	Al3Ni2	hP5	0.4028		0.4811	[37]
	AlNi	CsCl	cP2	0.28872			[35]
	Al3Ni5	Pt5Ga3	oC16	0.753	0.661	0.376	[35]
	AlNi3	Cu3Au	cP4	0.35792			[35]
	Al4Ni3	Ga4Ni3	cI112	1.144			[22]
Ni–Er	Er2Ni17	Th2Ni17	hP38	0.8287		0.8017	[22]
	Er5Ni22		hP108	0.4862		7.177	[22]
	Er4Ni17		hP126	0.4869		8.407	[22]
	ErNi4	PuNi4	mS30	0.4855	0.8444	1.0231	[22]
	Er2Ni7	Gd2Co7	hR54	0.4909		3.6067	[38]
	ErNi3	PuNi3	hR36	0.4941		2.4252	[30]
	ErNi2	MgCu2	cF24	0.71175			[31]
	Er3Ni2	Er3Ni2	hR45	0.8472		1.5680	[39]
	ErNi	FeB	oP8	0.6977	0.4110	0.5443	[39]
	Er3Ni	Fe3C	oP16	0.6804	0.9432	0.6245	[40]

System	Phase	Prototype	Pearson Symbol	Lattice Parameters (nm)			Refs.
				a	b	c	
Al–Er	Al3Er	AuCu3	cP4	0.4235			[26]
	Al2Er3	Al2Zr3	tP20	0.81323		0.75039	[41]
	AlEr2	Co2Si	oP12	0.6516	0.5015	0.9279	[42]
	AlEr	AlDy	oP16	0.55791	1.1277	0.5574	[43]
Al–Ni–Er							
τ1	Al19Ni5Er3	Al119Ni5Gd3	oS108	4.0565	15.8906	26.9752	[24]
τ2	Al9Ni3Er	Al9Ni3Er	hR78	7.2716		27.346	[44]
τ3	Al14Ni7Er3	Al14Ni7Gd3	hP72	17.8776		4.03212	[25]
τ4	Al4NiEr	YNiAl4	oS24	4.044	15.08	6.631	[22]
τ5	Al3−xNi2+xEr	Al3Ni2Y	hP18	9.01		4.049	[22]
τ6	Al2NiEr	MgCuAl2	oS16	4.064	10.06	6.898	[22]
τ7	AlNi8Er3	Ce3Co8Si	hP24	5.002		15.99	[22]
τ8	Al2Ni6Er3	Ce3Ni6Si2	cI44	8.88			[22]
τ9	AlNi2Er2	W2CoB2	oI10	5.347	8.374	4.157	[37]
τ10	AlNiEr	AlNiZr	hP9	6.970		3.8003	[45]
τ11	AlNiEr4						[34]
τ12	AlNi6Er13						[34]
τ13	AlNi2Er						[34]
τ14	Al12Ni2Er3						This work

References

1. Zhang, X.; Deng, Y.; Zhang, Y. Development of high strength aluminum alloys and processing techniques for the materials. Acta Metall. Sin. 2015, 51, 257–271.
2. Kong, Y.; Jia, Z.; Liu, Z.; Liu, M.; Roven, H.J.; Liu, Q. Effect of Zr and Er on the microstructure, mechanical and electrical properties of Al-0.4Fe alloy. J. Alloys Compd. 2020, 857, 157611.
3. Barkov, R.Y.; Mikhaylovskaya, A.; Yakovtseva, O.; Loginova, I.; Prosviryakov, A.; Pozdniakov, A. Effects of thermomechanical treatment on the microstructure, precipitation strengthening, internal friction, and thermal stability of Al–Er-Yb-Sc alloys with good electrical conductivity. J. Alloys Compd. 2020, 855, 157367.
4. Shang, Q.X.; Liu, Y.R.; Su, K.P.; Hu, S.L.; Wang, H.O.; Huang, S.; Yang, D.X.; Huo, D.X.; Liu, J. The Isothermal Section of the Al–Mn–In Ternary System at 773K and Hard Magnetic Properties of MnAlIn Alloys. J. Phase Equilibria Diffus. 2021, 42, 888–897.
5. Shen, Y.; Perepezko, J. Al-based amorphous alloys: Glass-forming ability, crystallization behavior and effects of minor alloying additions. J. Alloys Compd. 2017, 707, 3–11.
6. Yang, H.; Wang, J.; Li, Y. Influence of TM and RE elements on glass formation of the ternary Al–TM–RE systems. J. Non-Cryst. Solids 2008, 354, 3473–3479.
7. Abrosimova, G.; Aronin, A.; Budchenko, A. Amorphous phase decomposition in Al–Ni–RE system alloys. Mater. Lett. 2015, 139, 194–196.
8. Chang, Y.; Chen, S.; Zhang, F.; Yan, X.; Xie, F.; Schmid-Fetzer, R.; Oates, W. Phase diagram calculation: Past, present and future. Prog. Mater. Sci. 2004, 49, 313–345.
9. Deffrennes, G.; Joubert, J.-M.; Oudot, B. On models to describe the volume in the context of establishing high-pressure Gibbs energy databases. Calphad 2022, 78, 102435.

10. Pelton, A.D. Thermodynamics and phase diagrams of materials. In Phase Transformations in Materials; Wiley Online Library: New York, NY, USA, 2001; pp. 1–80.
11. Li, C.; Song, Q.; Yang, X.; Wei, Y.; Hu, Q.; Liu, L.; Zhang, L. Experimental Investigation of the Phase Relations in the Fe-Zr-Y Ternary System. Materials 2022, 15, 593.
12. Okamoto, H. Al-Ni (aluminum-nickel). J. Phase Equilibria Diffus. 2004, 25, 394.
13. Lee, K.J.; Nash, P. The Al-Ni-Ti system (Aluminum-Nickel-Titanium). J. Phase Equilibria Diffus. 1991, 12, 551–562.
14. Wang, Y.; Cacciamani, G. Thermodynamic modeling of the Al-Cr-Ni system over the entire composition and temperature range. J. Alloys Compd. 2016, 688, 422–435.
15. Gwyer, A.G.C. über die Legierungen des Aluminiums mit Kupfer, Eisen, Nickel, Kobalt, Blei und Cadmium. Z. Anorg. Chem. 1908, 57, 113–153.
16. Ansara, I.; Dupin, N.; Lukas, H.L.; Sundman, B. Thermodynamic assessment of the Al-Ni system. J. Alloys Compd. 1997, 247, 20–30.
17. Du, Y.; Clavaguera, N. Thermodynamic assessment of the Al□Ni system. J. Alloys Compd. 1996, 237, 20–32.
18. Huang, W.; Chang, Y. A thermodynamic analysis of the Ni-Al system. Intermetallics 1998, 6, 487–498.
19. Dupin, N.; Ansara, I.; Sundman, B. Thermodynamic re-assessment of the ternary system Al-Cr-Ni. Calphad 2001, 25, 279–298.
20. Lu, X.-G.; Sundman, B.; Ågren, J. Thermodynamic assessments of the Ni–Pt and Al–Ni–Pt systems. Calphad 2009, 33, 450–456.
21. Chen, H.-L.; Doernberg, E.; Svoboda, P.; Schmid-Fetzer, R. Thermodynamics of the Al3Ni phase and revision of the Al–Ni system. Thermochim. Acta 2011, 512, 189–195.
22. Ellner, M.; Kek, S.; Predel, B. ChemInform Abstract: Ni3Al4-A Phase with Ordered Vacancies Isotypic to Ni3Ga4. Less-Common Met. 1989, 154, 207–215.
23. Buschow, K. Crystal structures, magnetic properties and phase relations of erbium-nickel intermetallic compounds. J. Less Common Met. 1968, 16, 45–53.
24. Moreau, J.M.; Paccard, D.; Gignoux, D. The crystal structure of Er3Ni2. Acta Crystallogr. Sect. B Struct. Crystallogr. Cryst. Chem. 1974, 257, 195–209.
25. Du, Z.; Wang, D.; Zhang, W. Thermodynamic assessment of the Co–Pr, Er–Ni and Ni–Pr systems. J. Alloys Compd. 1999, 284, 206–212.
26. Buschow, K.H.J.; van Vucht, J.H.N. Das System Erbium-Aluminium und ein Vergleich mit dem System Yttrıum-Aluminium. Int. J. Mater. Res. 1965, 56, 9–13.
27. Gschneidner, K.A.; Calderwood, F.W. The Al−Er (Aluminum-Erbium) system. Bull. Alloy Phase Diagr. 1988, 9, 676–678.
28. Cacciamani, G.; Saccone, A.; De Negri, S.; Ferro, R. The Al-Er-Mg ternary system Part II: Thermodynamic modeling. J. Phase Equilibria 2002, 23, 38.
29. Xu, L.; Shi, X.; Xia, D.; Huang, D.; Tang, H. Experimental investigation and thermodynamic assessment of the Al–Er system. Calphad 2022, 79, 102482.
30. Zarechnyuk, O.; Rykhal, R.; Romaka, V.; Kovalska, O.; Shazabura, G. Isothermal sections of the Holmium, erbium-nickel-aluminium ternary systems at 800 °C in the 0 to 0.333 atomic fraction range of the rare-earth metal. Dop. Akad. Nauk Ukr. RSR Ser. A Fiz. Mat. Tekh. Nauki 1982, 14, 78–80.
31. Gladyshevskii, R.; Cenzual, K.; Parthé, E. The crystal structure of orthorhombic Gd3Ni5Al19, a new representative of the structure series R2+mT4+mAl15+4m. J. Solid State Chem. 1992, 100, 9–15.
32. Šorgić, B.; Drašner, A.; Blažina, Ž. The effect of aluminium on the structural and hydrogen sorption properties of ErNi5. J. Alloys Compd. 1996, 232, 79–83.
33. Riccardo, F.; Gilda, Z.; Rinaldo, M. Al-Er-Ni (aluminium–erbium–nickel). Landolt-Börnstein-Group IV Phys. Chem. 2005, 11A2, 249–256.
34. Zhao, F.; Zhang, L.; Wang, H.; Liu, L. Phase equilibria investigation of the Al–Ni–Er ternary system at 600 °C and 700 °C. Calphad 2021, 75, 102353.
35. Massalski, T.B.; Okamoto, H.; Subramanian, P.R. Binary Alloy Phase Diagrams, 2nd ed.; ASM International: Materials Park, OH, USA, 1990.
36. Viklund, P.; Haussermann, U.; Lidin, S. NiAl3: A structure type of its own? In Acta Crystallographica A-Foundation and Advances; Int Union Crystallography: Chester, UK, 1996; Volume 52, p. C321.

37. Bouche, K.; Barbier, F.; Coulet, A. Phase formation during dissolution of nickel in liquid aluminium. Zeitschrift Fuer Met. 1997, 88, 446–451.
38. Dwight, A.; Mueller, M.; Conner, R.; Downey, J.; Knott, H. Ternary compounds with the Fe2P-type structure. Trans. Am. Inst. Min. Metall. Pet. Eng. 1968, 242, 2075–2080.
39. Hilpert, K.; Kobertz, D.; Venugopal, V.; Miller, M.; Gerads, H.; Bremer, F.J.; Nickel, H. Phase Diagram Studies on the Al-Ni System. Ztschrift Für Nat. A 1987, 42, 1327–1332.
40. Delsante, S.; Richter, K.W.; Ipser, H.; Borzone, G. Synthesis and structural characterization of ternary compounds belonging to the series RE2+mNi4+mAl15+4m (RE = rare earth metal). Z. Für Anorg. Und Allg. Chem. 2009, 635, 365–368.
41. Buschow, K.; Van Der Goot, A. The crystal structure of rare-earth nickel compounds of the type R2Ni7. J. Less Common Met. 1970, 22, 419–428.
42. Dwight, A.E. The unit-cell constants of some PuNi3-type compounds. Acta Crystallogr. Sect. B Struct. Crystallogr. Cryst. Chem. 2010, 24, 1395–1396.
43. Wang, D.; Li, Y.; Long, Y.; Ye, R.; Chang, Y.; Wan, F. Hydrogen induced structural and magnetic transformations in magnetic regenerator materials ErNin (n = 1, 2) and HoCu2. J. Magn. Magn. Mater. 2007, 311, 697–701.
44. Okamoto, H.; Massalski, T.B. guidelines for binary phase diagram assessment. J. Phase Equilibria Diffus. 1993, 14, 316–335.
45. Garde, C.S.; Ray, J. Magnetic and superconducting behaviour of the (R = La, Pr, Gd, Tb, Ho and Er) systems. J. Phys. Condens. Matter 1997, 9, 7419–7434.